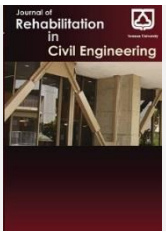

Journal of Rehabilitation in Civil Engineering

Journal homepage: https://civiljournal.semnan.ac.ir/

Designing the Soilbag Columns: An Analytical Approach and Numerical Validation

Abdollah Sadr [1]; Nader Hataf [2,*]

1. Department of Civil Engineering, University of Hormozgan, Bandar Abbas, formerly Department of Civil and Environmental Engineering, Shiraz University, Shiraz, Iran
2. Department of Civil and Environmental Engineering, Shiraz University, Shiraz, Iran

* Corresponding author: *nhataf@shirazu.ac.ir*

ARTICLE INFO

Article history:
Receive Date: 03 March 2023
Revise Date: 22 May 2023
Accept Date: 05 July 2023

Keywords:
Soilbag columns;
Analytical approach;
Numerical validation;
Design charts.

ABSTRACT

The use of wrapping geosystems such as soilbags as reinforcement has been increasingly studied. Soilbag columns may be utilized as an alternative method for improving the weak soil under the footing. An analytical approach was developed to predict the stress-strain response of the soilbags under compression. Using three-dimensional numerical modeling, the validity of the relationships was investigated and then developed for the soilbag columns supporting the footing loads. Compared to numerical results, it was found that for the stiffer wrapping materials, the analytical approach overestimates the bearing stress of the soilbag columns. However, the estimation of the bearing stress of soilbag columns matches well with the numerical results for high values of backfill friction angles. The results from the analyses were used to develop the design guidelines for the design of soilbag columns for the given settlement. Design charts propose a preliminary selection for the tensile stiffness of wrapping geosystems.

E-ISSN: 2345-4423

How to cite this article:
Sadr, A., & Hataf, N. (2024). Designing the Soilbag Columns: An Analytical Approach and Numerical Validation. Journal of Rehabilitation in Civil Engineering, 12(2), 14-25. https://doi.org/10.22075/jrce.2023.30079.1821

1. Introduction

The construction of permanent structures with soilbags has recently received attention [1]. Tatsuoka et al. [2] and Liu et al. [3] studied on the retaining walls formed by the soilbags. The Failure mechanism of the slopes and the embankments constructed by the soilbags has also been studied [4–6]. The application of soilbags as reinforcement has grown owing to a considerable increase in the bearing capacity of the granular materials by wrapping them with materials with appropriate tensile behavior, e.g., geotextiles [7]. When an external load is applied, soilbag tends to be flattened with an extension of the total perimeter, resulting in an induced tensile force (T) in the bag. This tension creates additional confining stresses that act on the infill materials inside the soilbags. The amounts of these stresses depend on the tension (T) developed in the wrapping materials and the bag dimensions [7,8]. Constraint dilatancy of the infill materials is also another factor affecting the bearing capacity of the soilbags [9]. The compressive behavior of the soilbags as reinforcement has been investigated experimentally by several researchers. Xu et al. [8] and Wang et al. [10] conducted a series of compression tests on the real-scale soilbags in the field and showed that soil improvement using soilbags significantly enhances the bearing capacity of weak soil as well as reduces settlement under applied loads. Wang et al. [10] attributed this to the generation of stress dispersion to the larger area through the soilbag reinforcement. Besides, Xu et al. [8] indicated that the horizontal pressure between the adjacent soilbags subjected to vertical loading is quite small. Lohani et al. [11] carried out a series of full-scale uniaxial compression as well as lateral shear tests on soilbag piles and investigated several parameters and concluded that the use of large aggregates as infill materials considerably increases the compressive strength of the soilbag piles.

Analytical methods have also been developed to predict the bearing capacity of the soilbags [7,8,12,13]. Tatsuoka [14] proposed an approximate isotropic perfectly plastic solution to predict the vertical compressive strength of the soilbag piles. Several numerical studies have been performed to better understand the behavior of the soilbags under external loads [12,15,16]. Using the discrete element method (DEM), Cheng et al. [9] and Liu et al. [17] modeled a soilbag under uniaxial and biaxial compression, respectively. Ansari et al. [12] using the finite element method investigated a soilbag subjected to compression and lateral cyclic shear loading. Tantono and Bauer [18] studied on the influence of the soil-geotextile interface in a soilbag using a hypo-plastic model. They also showed that the volumetric strain of the soilbag is very small. Numerical analyses were carried out by Doi et al. [19] to investigate the dynamic behavior of composite foundations composed of soilbags and piles. Haddad and Bahrehdar [20] using ABAQUS software, modeled a single soilbag under vertical compression. The results were in good agreement with experimental observations. They showed that bag thickness has an important role in the compressive strength of a soilbag.

Soilbag columns (SBCs) inserted beneath a footing as an alternative method of soil improvement technique has also been investigated [13]. Experimental and Numerical modeling of the soilbag columns located beneath a footing in a loose sand bed showed a substantial enhancement in bearing capacity compared to the encased stone columns [13,16].

There is very limited research on the application of soilbag columns to enhance the bearing capacity of weak foundations, also, no design guidelines are available for this new improvement technique. In the current study, using an analytical method verified by numerical simulations, design charts were prepared to provide a preliminary estimation

of the tensile stiffness of wrapping materials. The analytical and numerical approaches have been described in detail in the companion papers [13,16].

2. Analytical approach

2.1. Development of the stress-strain relationships for a single soilbag under compression

Fig.1 shows the principal stresses acting on the materials inside the square bag. These principal stresses can be computed using Eqs. (1) and (2) as follows:

$$\sigma_{1m} = \frac{\sigma_1(d' \times d') + 2T(d' + d')}{d' \times d'} = \sigma_1 + \frac{4T}{d'} \quad (1)$$

$$\sigma_{2m} = \sigma_{3m} = \frac{\sigma_3(d' \times t') + 2T(d' + t')}{d' \times t'} = \sigma_3 + 2T\left(\frac{1}{t'} + \frac{1}{d'}\right) \quad (2)$$

In this figure, σ_{1m}, σ_{2m} and σ_{3m} are the principal stresses, σ_1 and $\sigma_2 = \sigma_3$ are the external loads, and d' and t' are the width and height of the deformed soilbag, respectively. d and t are the initial width and height of the soilbag, respectively, and T is the tensile force induced in the geotextile.

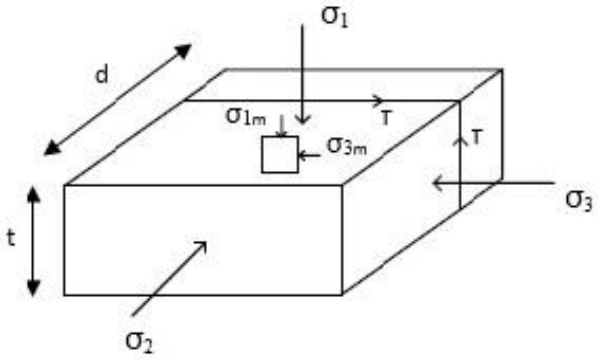

Fig. 1. Stresses acting on three-dimensional model soilbag and on particles inside the bag (after Sadr and Hataf, 2021).

The principal stress ratio of $\frac{\sigma_{1m}}{\sigma_{3m}}$ is related to the major principal strain ε_1 by Eq. (3) as:

$$\frac{\sigma_{1m}}{\sigma_{3m}} = f(\varepsilon_1)\ [1] \quad (3)$$

This ratio may be estimated using an exponential function proposed by Matsuoka and Liu [1] as Eq. (4):

$$f(\varepsilon_1) = C \cdot \exp(-\varepsilon_1) + K_p \quad (4)$$

where, $K_p = \frac{1+\sin\phi_b}{1-\sin\phi_b}$ is the passive earth pressure coefficient of the infill materials, φ_b is the friction angle of infill materials, and C is a coefficient depends on the initial state of the materials inside the soilbag. Matsuoka and Liu [1] showed that $C=1-K_p$ for isotropic state.

Sadr and Hataf [13] derived Eq. (5), an expression to relate the external loads to the principal strain (ε_1), as:

$$\sigma_1 = \sigma_3 f(\varepsilon_1) + \frac{2J}{d'}\left\{\left[(1-\varepsilon_1)\cdot\frac{m'+1}{m+1} - 1\right]\cdot [f(\varepsilon_1)(m'+1) - 2]\right\} \quad (5)$$

where, J is the tensile stiffness of the wrapping material and $m = \frac{d}{t}$. m and m' were related using Eq. (6) as:

$$m' = \frac{m}{(1-\varepsilon_1)^{3/2}} \quad (6)$$

The width of each soilbag after deformation (d') was obtained using Eq. (7) and with the assumption of constant volume:

$$d' = \frac{d}{\sqrt{1-\varepsilon_1}} \quad (7)$$

Tantono and Bauer [18] and Cheng et al. [9] stated that the soilbags deform under small volumetric change. The stress–strain relationship predicted by Eq. (5) matched well with the results of uniaxial compression test [13].

2.2. Estimation of the compressive strength of a SBC and numerical validation

Numerical simulations using ABAQUS were conducted to investigate the compressive behavior of a SBC beneath a rigid footing [16]. It was found that 3D modeling of a SBC is quite intricate. The material contained in the

soilbags and the surrounding loose sand was characterized using a linearly elastic, perfectly plastic model with a Mohr Coulomb failure criterion and non-associated flow rule. Square soilbags, measuring 54 cm by 54 cm by 10 cm, were numerically modeled and combined to form a SBC. The chosen width-height ratio is identical to that used in previous studies of soilbags [7,10] and is more representative of actual field applications. The geometry of all SBCs and ESCs modeled and analyzed in the present study was assumed to have two symmetry planes. Thus, to reduce computational effort, only one-quarter of the actual solution domain, consisting of the SBC and surrounding loose sand, was modeled. To properly account for the aforementioned planes of symmetry, displacements were prevented in a direction normal to such planes. Along the lateral boundaries, displacements were constrained in the global x and y-coordinate directions (Fig. 2). All SBCs modeled as part of the present study were assumed to reach a firm stratum, i.e., they were end-bearing. Consequently, along the bottom (x-y) plane, displacements in the global z-direction were prevented. The interfaces at the contacts should also be well-defined. In modeling the bag-soil and bag-bag interactions, two distinct contact surfaces were defined. They were modeled using the surface-to-surface finite sliding formulation. To accurately simulate the interfaces between the geosynthetic and the encased soil and between the geosynthetic and the surrounding soil, a "hard" contact and a "penalty" approach were used to simulate the normal and tangential response, respectively. The former ensures that the penetration along soil-geosynthetic interfaces will be minimized. It is timely to note that the use of surface-to-surface interfaces has been shown to reduce the "hourglass effects" that can potentially affect the performance of reduced integration elements. To determine the stress-settlement response of such a SBC, an area consisting of the entire cross-section of the column and a portion of the surrounding soil (commonly referred to as the "loading area") was subjected to a series of prescribed vertical displacements. The maximum displacement was assumed to be 15 cm, i.e., 25% of the diameter of an ESC. For all models, the ARR was kept constant at 14.5%. Large number of contacts in a SBC results in considerably increase in computing time cost. Fig.2 depicts an end-bearing SBC modeled in the software. Numerical modeling was verified with the experimental measurements. Simulated stresses were slightly smaller than that for experimental ones [16]. The results indicated that the internal friction angle of the infill materials and the wrapping materials stiffness are the major parameters affecting the compressive strength.

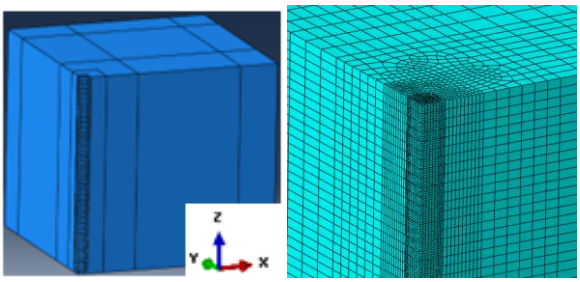

Fig. 2. Modeling of a SBC; geometry (left) and meshing pattern (right).

For instance, an increase in φ_b from 40° to 44° resulted in increase in the bearing stress of the SBCs by 36%. In particular, changing J from 100 to 2000 kN/m increased the stress in the SBCs by a factor of 11 [16]. Hence, the variations of these parameters were predicted by the proposed analytical expressions, then compared with those simulated by the software.

The entire load carried by the column is supported by the first soilbag, then it is transmitted along the column. So, the uppermost soilbag essentially determines the compressive strength of the SBCs. The total displacement applied to a SBC is transmitted along the column and shared among the soilbags. To use Eq. (5), knowing the vertical strain ($\mathcal{E}_1$) of the first soilbag is essential. The vertical deformation of the first soilbag

obtained by the numerical modeling was employed in Eq. (5).

Fig. 3 depicts a comparison between the numerical and analytical solutions for the SBCs with varied ϕ_b and wrapping materials stiffness (J). These results were obtained by applying $C=1-Kp$ and $\sigma_3=0$. As seen, for the stiffer wrapping materials, the analytical approach overestimated the bearing stress of the SBCs. To derive the expressions, some assumptions were made [13], including the uniformity of the tensile stress (T) induced in wrapping materials. Since the tensile stress is not really uniform throughout the bag, the predictions overestimate additional confining stresses. In contrast, the estimation of the bearing stress of the SBCs matched well with the numerical results for higher values of backfill friction angles.

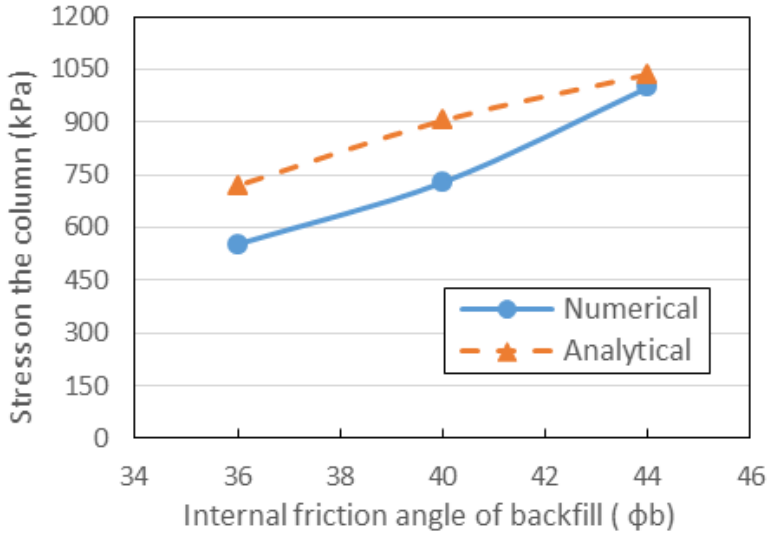

(a)

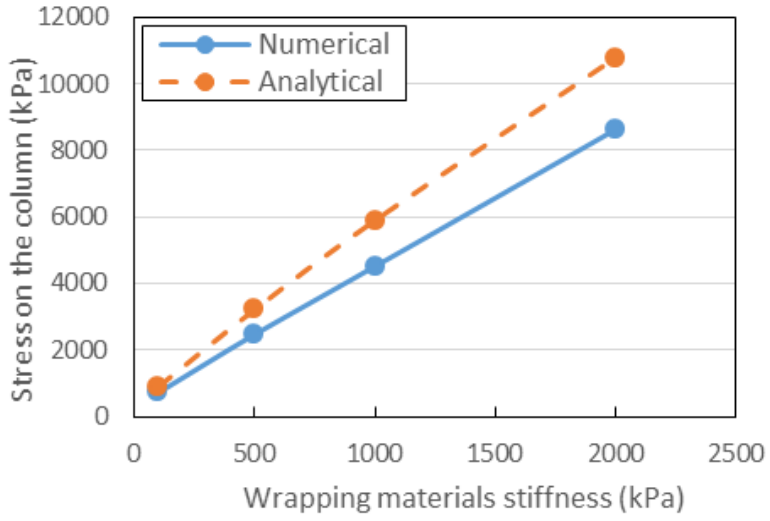

(b)

Fig. 3. Comparison between analytical and numerical results of SBCs; (a) varied friction angle of backfill (φ_b) and (b) varied wrapping materials stiffness (J).

Fig. 3 indicates that for the SBCs with high values of J, the effect of wrapping material stiffness is quite dominant. Hence, to investigate the influence of the internal friction angle of the infill materials (φ_b), J=100 kN/m, i.e., a small value for wrapping materials

stiffness was employed. The vertical stresses for varied wrapping materials stiffness (Fig. 3(b)) were predicted with $\varphi_b = 40°$.

2.3. Correction factors

Since the predictions obtained by Eq. (5) were overestimated compared to numerical results (fig.3), two correction factors of I_1 and I_2 related to different values of J and φ_b, respectively, were introduced. They were computed based on the numerical results as a benchmark. To compute I_1 and I_2, the values of the friction angle of infill materials and stiffness of the wrapping material were kept constant, respectively. These correction factors are as follows:

For $J > 100$ kN/m $I_1 = 1.30$

For $\varphi_b = 36°$ and $J = 100$ kN/m $I_2 = 1.30$

For $\varphi_b = 40°$ and $J = 100$ kN/m $I_2 = 1.20$

For $\varphi_b = 44°$ and $J = 100$ kN/m $I_2 = 1.00$

To determine the appropriate correction factors for different combinations of φ_b and J, six cases of SBCs with different properties were modeled in ABAQUS. The stresses on the column (σ_c) at the corresponding normalized settlement (S_e/t) were presented in the table. 1. S_e is the amount of applied settlement. The values illustrated in this table indicate that $I_1.I_2$ may be adopted as an appropriate correction factor ($C.F$). Therefore, Eq. (5) was corrected by applying the correction factor as Eq. (8):

$$\sigma_{1(\text{corrected})} = \frac{\sigma_1}{\text{C.F}} \quad (8)$$

where, σ_1 is computed using Eq. (5) and $C.F = I_1.I_2$. The aforementioned equation was used to prepare the design charts in the next section.

2.4. Design guidelines

Based on the results obtained by the analytical approach, the following guidelines were suggested to design the SBCs. Design charts have been prepared in a non-dimensional form and for three values for φ_b and two values for d/t (Figs. 4 and 5). To use the proposed design charts, the following steps should be considered:

Step 1. First of all, for the given pressure loading from the structure (σ_0), appropriate spacing (s) and width of the SBCs are chosen.

Step 2. The allowable settlement (S_{all}) is normalized with the height (t) of each soilbag (x-axis).

Step 3. For the known pressure from the structure to the foundation (σ_0), the stress applied on each column is calculated. It is assumed that all the external load is transferred to the columns, and the contribution of the surrounding soil was conservatively ignored. According to the unit cell concept, the value of column load can be computed using Eq. (9) as:

$$\text{Pc} = \sigma 0 \,.\, \text{A} \quad (9)$$

where, P_c is the column load and A is the unit cell area. The value of A is attributed to the column arrangement in the group. For triangular pattern: $A = \pi \times (0.525s)^2$ and for square pattern: $A = \pi \times (0.564s)^2$ where S is the spacing of the columns. Stress on the columns, then, is calculated using the following expression:

$$\sigma_c = P_c / A_c \quad (10)$$

where, σ_c is the stress on the column and A_c is the column cross-section area.

Step 4. For a friction angle of the infill materials (φ_b) and the allowable settlement (S_{all}), normalized wrapping materials stiffness ($\frac{J}{\sigma_c.d}$) is determined by the chart (Y-axis). d is the width of the soilbag forming the column. Linear interpolation may be needed for other values of φ_b or d/t.

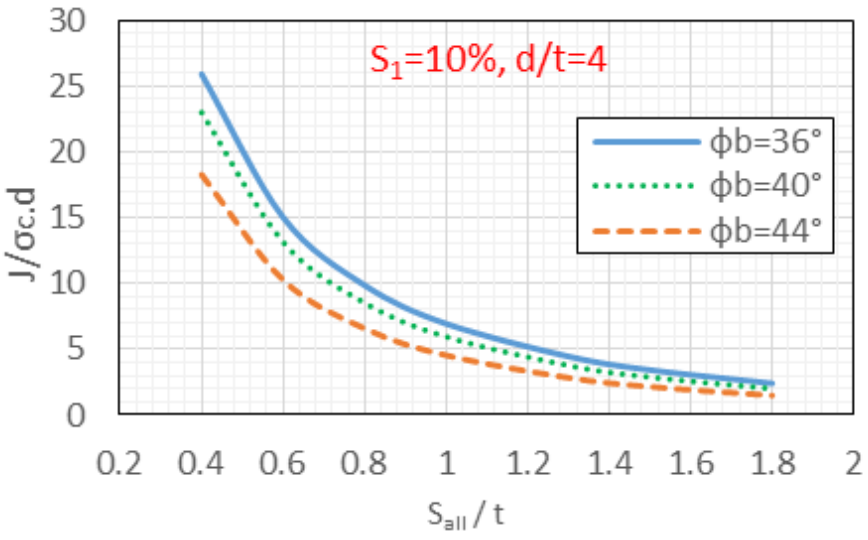

(a)

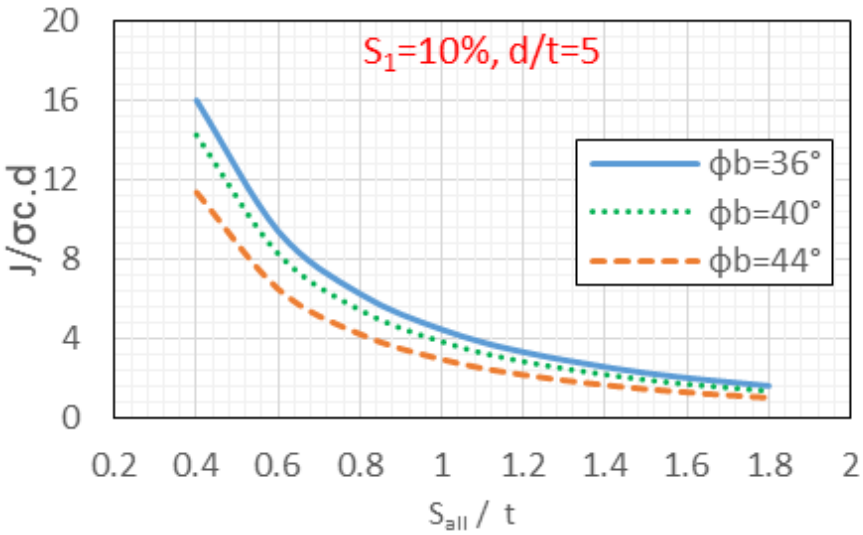

(b)

Fig. 4. Design charts for varied φb and S1=10%; (a) d/t=4 and (b) d/t=5.

Table1. Comparison of different cases with varied J, φ_b and S_e/t.

x	φ_b (°)	J (kN/m)	S_e/t	$\frac{\sigma_{(c)analytical}}{\sigma_{(c)numerical}}$	$C.F=I_1.I_2$	Difference(%)
1	36	2000	0.7	1.55	1.69	9.03
2	36	4000	1.2	1.50	1.69	12.67
3	40	2000	0.6	1.44	1.56	8.33
4	40	2500	1.0	1.42	1.56	9.85
5	44	1500	0.5	1.27	1.3	2.36
6	44	3000	1.5	1.25	1.3	4.00

Step 5. By using the given σ_0, as well as the normalized tensile stiffness (calculated from the previous step), a preliminary selection for tensile stiffness (J) of the wrapping materials can be proposed.

The effect of σ_3 in the Eq. (8) was ignored, hence, the proposed design charts for the SBCs

are conservatively applicable for all values of friction angle of the surrounding soil.

To compute the column stress (σ_c) using Eq. (8), it is necessary to know the amount of vertical deformation of the uppermost soilbag. In the current numerical study, the maximum settlement applied to the columns was S_e=1.8t and the maximum ratio of the vertical deformation of the uppermost soilbag to the applied settlement (S_1) was 17%.

At the initial steps of loading in which the amounts of the settlement were really small, S_1 was nearly 3%. However, for a range of $0.4 \leq S_e/t \leq 1.8$, this value put between 10% to 17%. The design charts were prepared for S_1 = 10% and 17% of the allowable settlement and d/t = 4 and 5.

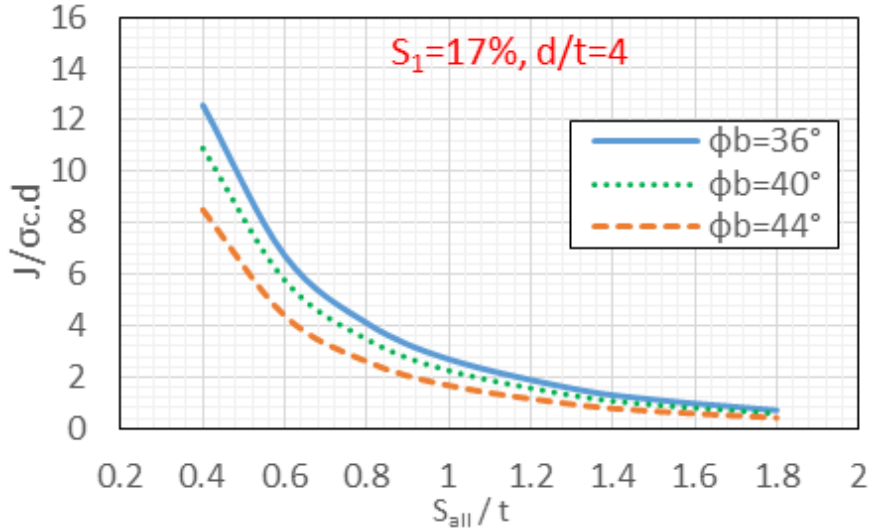

(a)

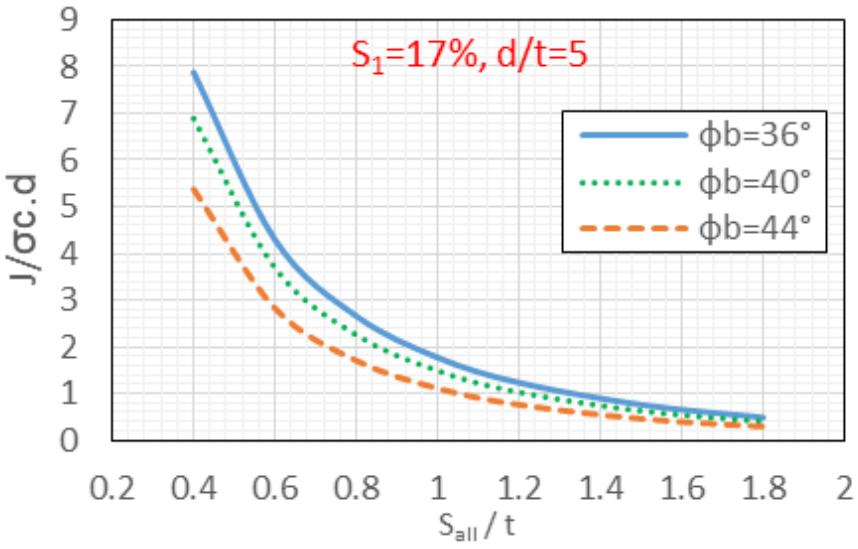

(b)

Fig. 5. Design charts for varied φ_b and S1=17%; (a) d/t=4 and (b) d/t=5.

3. Worked example

In this section, a design example using the charts proposed in the previous section is presented.

Matsuoka and Liu [1] presented case studies of using soilbags as reinforcement. They stated that the standard size of the soilbags was 40 cm and 10 cm in width and height, respectively. The same dimensions were used in this example. It is assumed that the column

is formed of four soilbag in each cross-section. Therefore, the width of the column is equal to 80 cm. Cheng et al. [9] showed that the dilatancy of the materials inside the smaller bags is better constrained. Thus, the use of smaller soilbags increases the advantage of using more dilative materials to improve the compressive strength of the SBCs. Therefore, the use of four soilbag with d=40 cm is preferred to a single soilbag with 80 cm. The columns formed of four soilbags adjacent to each other have been performed in the practice [1]. Regarding the spacing of the SBCs in a group, there is no information in the literature. In an encased stone column (ESC), the compressive strength of the encased soil enhances due to the confining effect of the tensile stress induced in the geotextile. This mechanism is similar to what occurs in a soilbag. So, in the absence of any information about the spacing parameter in an SBC group, using the value that is commonly chosen for the ESCs may be a reasonable idea. Rao et al. [21] and Ambily and Gandhi [22] found no significant improvement when the spacing is greater than 3d. Alexiew et al. [23] recommended a range of 1.5m to 2.5m for the spacing of the ESCs. In this regard, a value of 1.75 m was chosen. The structures supported by the geo-columns (ESCs, SBC, …) are often less sensitive to settlement [24]. An allowable settlement equal to 10 cm was used in this example. In this example, it is assumed a triangular pattern, so, $A=\pi\times(0.525s)^2$ =2.65 m^2.

The value of pressure from the structure to the foundation was assumed to be 1.5 kg/cm^2 or 150 kPa. The column load is computed as:

$P_c= \sigma_0 .A= 398$ kN.

and stress on the column is:

$\sigma_c=P_c/A_c = 398/(0.8)^2= 622$ kPa.

Using Figs 4(a) and 5(a) and for φ_b=44° and $\frac{S_{all}}{t}=1$, the upper and lower values of wrapping materials stiffness (J) can be estimated to be 1100 kN/m and 420 kN/m, respectively.

4. Conclusions

Design guidelines for soilbag columns were prepared based on an analytical approach developed for the soilbags under compression. In Comparison with the numerical simulations of the SBCs, the proposed computational method was overestimated, especially for stiffer wrapping materials. Hence, the correction factors were introduced and applied to the analytical predictions. knowing the pressure loading from the structure and the allowable settlement, the design charts enable the designers to have a preliminary estimation for the tensile stiffness of the wrapping materials (J). These values may yield the upper and lower estimations for selecting the stiffness of the wrapping materials. The aforementioned charts were prepared for S_I = 10% and 17% of the allowable settlement. The ratios of width to height of each soilbag were equal to 4 and 5. It is worth noting that the numerical data used to prepare the charts were reported from the modeling of the soilbag columns with a maximum value of settlement equal to S_e=1.8t. For the cases with larger amounts of settlement, the proposed charts may be used with caution.

Acknowledgments

Numerical studies of this paper were conducted during a research stay program at the Department of Civil and Environmental Engineering, University of Delaware (USA).

The first author expresses his gratitude to Prof. Kaliakin and Prof. Manahiloh for their significant scientific contributions.

Notations

A= unit cell area

A_c= column cross-section area

C= a coefficient depends on the initial state of the materials inside the soilbag

$C.F$= correction factor for preparing design charts

d= soilbag width

d'= soilbag width after deformation

I_1 and I_2= Correction factors correspond to J and ϕ_b, respectively

J= tensile stiffness of the wrapping materials

K_p= passive earth pressure coefficient of the infill materials

P_c= Column load

S= spacing of the columns in a group

S_1= Ratio of the vertical deformation of the uppermost soilbag to the applied settlement

S_e= applied settlement

S_{all}= allowable settlement

SBC= soilbag column

T= tensile force developed in the bag

t= initial height of the soilbag

t'= height of the soilbag after deformation

σ_0= pressure from the structure to the foundation

σ_{1m}, σ_{2m} and σ_{3m}= principal stresses acting on the particles inside the bag

σ_1, σ_2 and σ_3= external stresses

$\sigma_{1(corrected)}$= corrected vertical stress (σ_1)

ε_1= major principal strain (vertical direction)

ϕ_b= friction angle of infill materials

Funding

This research did not receive any specific grant from funding agencies in the public, commercial, or not-for-profit sectors.

Conflicts of interest

The author (N. Hataf) is an Editorial Board Member for Journal of Rehabilitation in Civil Engineering and was not involved in the editorial review or the decision to publish this article.

Authors contribution statement

Abdollah Sadr: Formal analysis; Investigation; Resources; Methodology; Software; Validation; Writing – review & editing

Nader Hataf: Conceptualization, Supervising, Reviewing and editing the article.

References

[1] Matsuoka, H; Liu S. A new earth reinforcement method using soilbags. CRC press; 2006.

[2] Tatsuoka F, Tateyama M, Uchimura T, Koseki J. Geosynthetic-Reinforced Soil Retaining Walls as Important Permanent Structures 1996 - 1997 Mercer Lecture. Geosynth Int 1997;4:81–136. https://doi.org/10.1680/gein.4.0090.

[3] Liu S, Fan K, Xu S. Field study of a retaining wall constructed with clay-filled soilbags. Geotext Geomembranes 2019;47:87–94. https://doi.org/10.1016/j.geotexmem.2018.11.001.

[4] Huang C-C, Matsushima K, Mohri Y, Tatsuoka F. Analysis of sand slopes stabilized with facing of soil bags with extended reinforcement strips. Geosynth Int

- GEOSYNTH INT 2008;15:232–45. https://doi.org/10.1680/gein.2008.15.4.232.

[5] Matsushima K, Tatsuoka F, Mohri Y, Aqil U. Shear strength and deformation characteristics of geosynthetic soil bags stacked horizontal and inclined. Geosynth Int - GEOSYNTH INT 2008;15:119–35. https://doi.org/10.1680/gein.2008.15.2.119.

[6] Xu Y, Zhang H. Design of soilbag-protected slopes in expansive soils. Geotext Geomembranes 2021;49:1036–45. https://doi.org/https://doi.org/10.1016/j.geotexmem.2021.02.001.

[7] Matsuoka H, Liu S. New Earth Reinforcement Method by Soilbags ("Donow"). Soils Found 2003;43:173–88. https://doi.org/https://doi.org/10.3208/sandf.43.6_173.

[8] xu Y, Huang J, Du Y, Sun D. Earth reinforcement using soilbags. Geotext Geomembranes - GEOTEXT Geomembr 2008;26:279–89. https://doi.org/10.1016/j.geotexmem.2007.10.003.

[9] Cheng H, Yamamoto H, Thoeni K. Numerical study on stress states and fabric anisotropies in soilbags using the DEM. Comput Geotech 2016;76:170–83. https://doi.org/https://doi.org/10.1016/j.compgeo.2016.03.006.

[10] Wang L, Liu S, Liao J, Fan K. Field load tests and modelling of soft foundation reinforced by soilbags. Geosynth Int 2019;26:1–36. https://doi.org/10.1680/jgein.19.00036.

[11] Lohani T, Matsushima K, Aqil U, Mohri Y, Tatsuoka F. Evaluating the strength and deformation characteristics of a soil bag pile from full-scale laboratory tests. Geosynth Int - GEOSYNTH INT 2006;13. https://doi.org/10.1680/gein.2006.13.6.246.

[12] Ansari Y, Merifield R, Yamamoto H, Sheng D. Numerical analysis of soilbags under compression and cyclic shear. Comput Geotech 2011;38:659–68. https://doi.org/10.1016/j.compgeo.2011.02.002.

[13] Sadr A, Hataf N. Experimental and analytical study on soilbag and encased sand columns in loose sand. Transp Geotech 2021;29:100553. https://doi.org/https://doi.org/10.1016/j.trgeo.2021.100553.

[14] Tatsuoka F. An approximate isotropic perfectly plastic solution for compressive strength of geosynthetic-reinforced soil. Geosynth Int - GEOSYNTH INT 2004;11:390–405. https://doi.org/10.1680/gein.2004.11.5.390.

[15] Hataf N, Sayadi M. Experimental and numerical study on the bearing capacity of soils reinforced using geobags. J Build Eng 2017;15. https://doi.org/10.1016/j.jobe.2017.11.015.

[16] Sadr A, Kaliakin VN, Hataf N, Manahiloh KN. Numerical study of soilbag columns and comparison to encased soil columns in loose sand. Comput Geotech 2022;142:104588. https://doi.org/https://doi.org/10.1016/j.compgeo.2021.104588.

[17] Liu S-H, Jia F, Shen C-M, Weng L-P. Strength characteristics of soilbags under inclined loads. Geotext Geomembranes 2018;46:1–10. https://doi.org/https://doi.org/10.1016/j.geotexmem.2017.09.002.

[18] Tantono SF, Bauer E. Numerical simulation of a soilbag under vertical compression, 2008.

[19] Doi T, Murono Y, Iwai H, Zhang F. Numerical investigation of dynamic behavior of composite foundation composed of soilbags and piles by 3D elastoplastic FEM. Soils Found 2022;62:101158. https://doi.org/https://doi.org/10.1016/j.sandf.2022.101158.

[20] Haddad A, Bahrehdar M. Numerical and experimental evaluation of soilbags deformation under vertical loading, 2012.

[21] Rao, S.N; Reddy, K.M; Kumar PH. Studies on groups of stone columns in soft clays. Geotech Eng J South East Asian Geotech Soc 1997;28:165–82.

[22] A.P. A, Gandhi S. Behavior of Stone Columns Based on Experimental and FEM Analysis. J Geotech Geoenvironmental Eng - J GEOTECH GEOENVIRON ENG 2007;133. https://doi.org/10.1061/(ASCE)1090-0241(2007)133:4(405).

[23] Dr. Alexiew D, Brokemper D, Lothspeich S. Geotextile Encased Columns (GEC): Load Capacity, Geotextile Selection and Pre-Design Graphs. Geotech. Spec. Publ., 2005, p. 1–14. https://doi.org/10.1061/40777(156)12.

[24] Shahu JT, Madhav MR, Hayashi S. Analysis of soft ground-granular pile-granular mat system. Comput Geotech 2000;27:45–62. https://doi.org/https://doi.org/10.1016/S0266-352X(00)00004-5.